



encit 2020



18th Brazilian Congress of Thermal Sciences and Engineering
November 16-20, 2020 (Online)

ENCIT-2020-0161

TECHNICAL, ECONOMIC AND ENVIRONMENTAL GEOREFERENCED ASSESSMENT OF PHOTOVOLTAIC SYSTEMS

João Henrique Paulino de Azevedo

Sergio Leal Braga

Department of Mechanical Engineering, Pontifical Catholic University of Rio de Janeiro (PUC-Rio).

22451-900. Rio de Janeiro – RJ. Brasil.

joao.hpa@hotmail.com; slbraga@puc-rio.br

Abstract.

This work aims to develop a program for simulation and generation of georeferenced maps that indicate the business opportunities for photovoltaic systems in a given area/ region, in order to serve investors and future beneficiaries of distributed generation. For this, a robust algorithm was developed that uses several equations in the literature to estimate incident radiation and energy generated by a photovoltaic system. Global solar radiation, wind speed and temperature data are obtained from maps generated by 39 solarimetric stations within and near the borders of the state of Rio de Janeiro. A methodology was implemented to analyze the technical, financial and environmental feasibility of photovoltaic systems. After a series of validations and sensitivity analysis, the simulation tool presented satisfactory results in terms of its forecasting capacity. The results reveal the simulation tool capacity to generate georeferenced maps for several indicators, which allow the investor to have greater power in making decisions for their investments in photovoltaic solar energy.

Keywords: solar energy; solar radiation; photovoltaic systems sizing; economic analysis; solarimetric maps

1. INTRODUCTION

With the need for greater diversification of the world energy matrix and the inevitability of investing in clean energy sources aiming at a lower emission of greenhouse gases, photovoltaic solar energy has been one of the most promising energy source, due to its potential and capacity electricity production. Its growth today is exponential and is increasingly present in the energy matrix of most countries. In Brazil, there is already a solid photovoltaic market with the generation of thousands of jobs and investments of billions of reais. According to the Energy Research Office (EPE) in 2029 there will be 1.3 million adopters of distributed photovoltaic micro or mini-generation systems, totaling 11.4 GW, which will require almost R\$ 50 billion in investments over the period (MME/EPE, 2020).

Its intermittency and unpredictability is the reason for great research, in order to obtain reliable data that estimate the generation of a photovoltaic solar system throughout its life cycle. Having more accurate data and closer to the generation reality, it is possible to carry out a more reliable economic-financial analysis of a photovoltaic project, which is essential for the study and comparison of feasibility between different projects. The investor lacks defined and grounded information for investment decisions within states or small regions, as the literature lacks this information. The information released today in the form of maps is generally radiation and local generation, but this cannot be a decisive factor for the viability of a project. Therefore, developing a tool for generating georeferenced maps, with feasibility indicators for photovoltaic projects is essential for investors and future beneficiaries of distributed generation.

2. COMPUTATIONAL MODEL

The simulation tool was developed in MATLAB platform. Figure 1 shows the simplified routine of the computational model. The first step is to specify the geographic coordinate, latitude and longitude, from where the photovoltaic solar energy project is to be installed. In addition, it is possible for the user to enter the project's monthly energy consumption so that the system is dimensioned according to consumption. It is also necessary to choose which model of photovoltaic module and inverter that will be used in the system, available in an extensive database.

With the geographic coordinate, it is possible to choose daily average monthly radiation, wind speed and temperature or hourly data obtained directly from one of the 35 specified INMET (The Brazilian National Institute of Meteorology) stations (CABRERA, 2014). When using daily average monthly data, one of the six correlations must be used to transform them into hourly data (COLLARES-PEREIRA; RABL, 1979; GARG; GARG, 1987; GUEYMARD,

1986, 2000; NEWELL, 1983; WHILLIER, 1956). Also with the coordinates, it is possible to calculate all the angles of solar positioning (IQBAL, 1983; SPENCER, 1971).

Thus, the correlation of Erbs et al. (1982), is used to calculate the diffuse and direct radiation incident on a horizontal surface (ERBS; KLEIN; DUFFIE, 1982). In the next step, the user can choose between four different configurations of solar tracking: fixed, one vertical axis, one axis with fixed inclination and two axes (BRAUN; MITCHELL, 1983). To calculate the diffuse radiation incident on the inclined surface, it is necessary to choose one of the three models available (REINDL; BECKMAN; DUFFIE, 1990)(REINDL; BECKMAN; DUFFIE, 1990)(REINDL; BECKMAN; DUFFIE, 1990)(REINDL; BECKMAN; DUFFIE, 1990)(LIU; JORDAN, 1963; PEREZ et al., 1990; REINDL; BECKMAN; DUFFIE, 1990).

Inverter and photovoltaic module technical data are obtained from database provided by the California Energy Commission (CEC). In this paper, the performance of the photovoltaic module is then calculated by (DUFFIE, J. A.; BECKMAN, 2020) model. The calculation of the energy tariff is necessary, as it varies according to location and consumption. Finally, with a robust algorithm for economic and financial analysis it is possible to calculate the feasibility indicators (NATURAL RESOURCES CANADA, 2005; SHORT; PACKEY; HOLT, 1995).

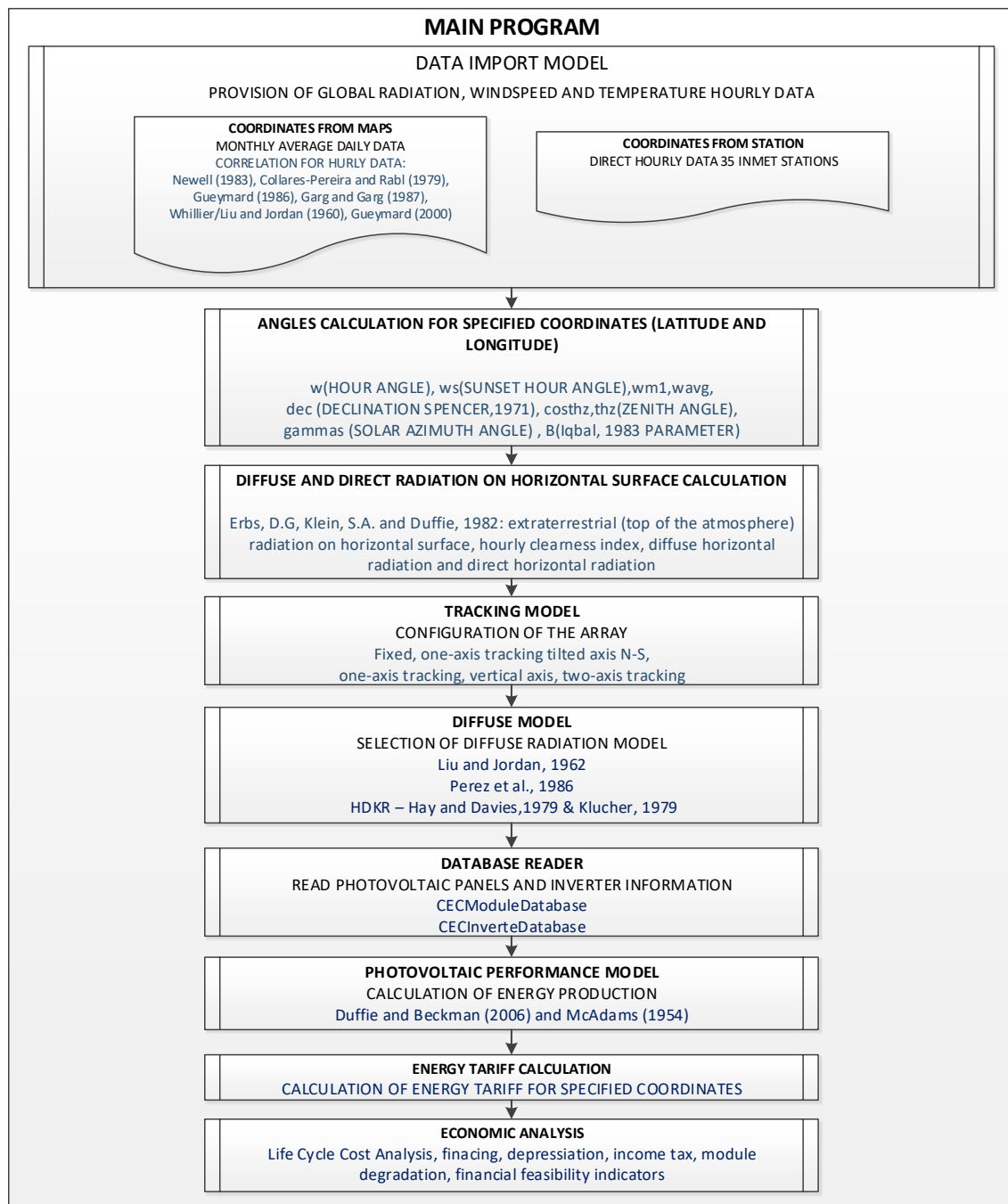


Figure 1 – Simulation tool computational routine.

For the generation of georeferenced maps of feasibility indicators, this calculation is performed for each of the geographic coordinates of the computational mesh within the geographic limit of the state of Rio de Janeiro. Figure 2 represents the computational mesh used in this work and the energy distributors concession areas. Each blue dot represents the point from which the calculations are made. This mesh corresponds to 7577 divided points equally located in the interior of the state of Rio de Janeiro. The ArcGIS platform was used to delimit the borders of Rio de Janeiro and the concession districts of the energy distributors, which influence the adopted energy tariff.

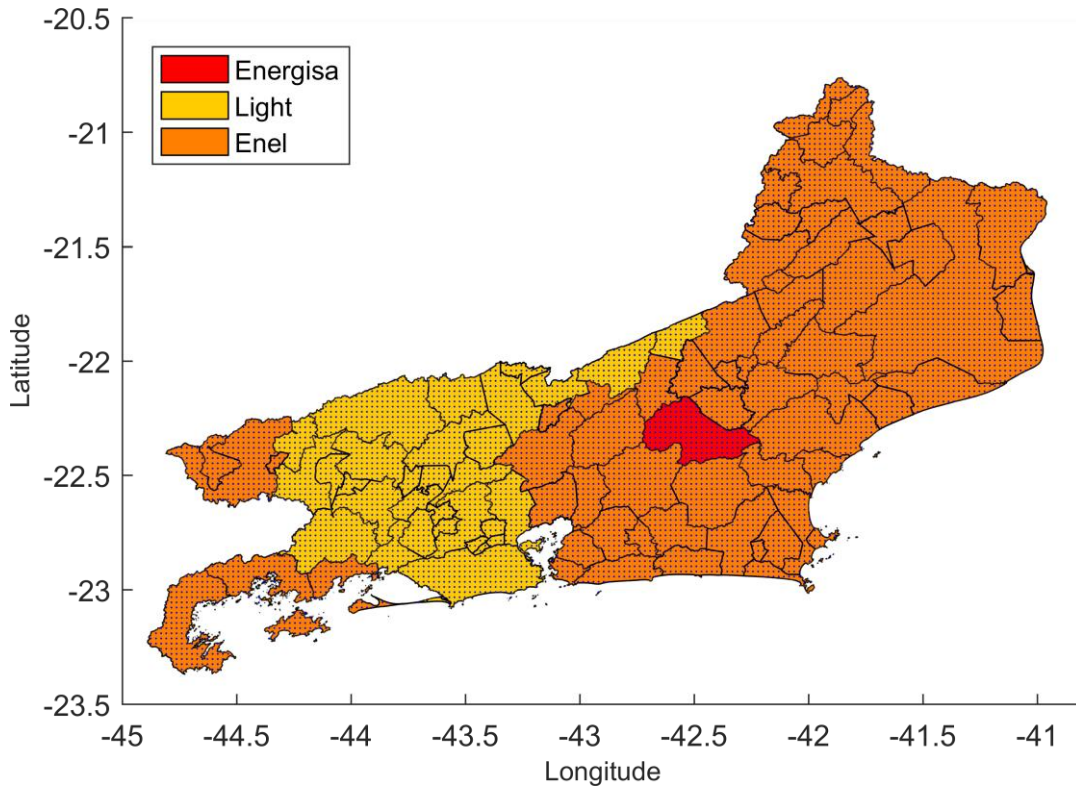


Figure 2 – Energy distributors concession areas and computational mesh for Rio de Janeiro state.

2.1 Photovoltaic system sizing

For dimensioning the power of the system, it is important to have an understanding of the compensation system regulated by the country. The Brazilian Electricity Compensation System uses what is commonly known as “net metering” (ANEEL, 2017). A bidirectional meter is installed and when the photovoltaic system generates more energy than demanded by the consumer installation, the surplus energy is delivered to the electrical network and the meter records this energy. The opposite occurs when the building consumes more energy than that generated by the PV system, causing the meter to register the flow in its conventional direction in this case.

It is not interesting that the photovoltaic system generates, over the year, more energy than that consumed by the consumer unit, as long as there is no possibility of shared generation, that is, to assign credits to other consumer units. Likewise, it is necessary to take into account the charge for the availability cost charged every month. Thus, this work measures the power of the photovoltaic system according to the following equation:

$$CON_a = \sum_{i=1}^{12} CON_{m_i} \quad (1)$$

$$CON_{dim} = CON_a - 12 * C_{disp} \quad (2)$$

Where CON_{m_i} corresponds to the monthly electricity consumption of month i , CON_a the total annual electricity consumption, C_{disp} the cost of availability and CON_{dim} the dimensioning consumption. To determine the power of the system, an iteration is performed for the number of panels used. When the energy generated by the system reaches the dimensioning consumption, the power is defined.

2.2 Economic-financial analysis

This section describes the process and equation used to carry out the economic-financial analysis of photovoltaic solar energy projects. The procedure used in the simulation tool is based on the NREL methodology (SHORT; PACKEY; HOLT, 1995) and the RETScreen software (NATURAL RESOURCES CANADA, 2005). This analysis is considered to be of paramount importance, as it reveals essential economic indicators for analyzing the feasibility of energy generation projects in general.

For a photovoltaic solar energy project, the initial cost of project C can be priced at the cost in R\$ of installed kWp practiced in the Brazilian market. (GREENER, 2020), carried out a market survey interviewing 884 photovoltaic system installation companies in Brazil. The survey confidence is 95% with a margin of error of 5%. Also, (PORTAL SOLAR, 2020) is the largest solar energy marketplace in Brazil, which brings together more than 1300 companies in the sector and provides information on the average costs charged for installing photovoltaic systems, based on the budgets offered by companies on the portal.

From the database of these two references, empirical equations were generated that represent the initial cost of a project according to the system power. It was possible to generate linear equations divided by a power range with a determination coefficient R^2 greater than 99% and an error margin of $\pm 2.55\%$:

$$C(P_s) = \begin{cases} 3613,2P_s + 6481,9, & P_s < 15 \text{ (RESIDENCIAL)} \\ 3299,3P_s + 10697, & 15 \leq P_s < 75 \text{ (COMERCIAL)} \\ 3305P_s + 10075, & 75 \leq P_s < 500 \text{ (INDUSTRIAL)} \\ 3043,5P_s + 161576, & 500 \leq P_s < 5000 \text{ (INDUSTRIAL II)} \end{cases} \quad (3)$$

where P_s is the system power in kWp. The suggested power ranges are according to the size of the project and can be classified respectively as: residential, commercial, industrial and industrial II.

In addition, (GREENER, 2020a) also provides data on the installment price portion that properly corresponds to the solar photovoltaic system kit and the company's installation service. This data is important for estimating which portion of the initial cost will be depreciable or not.

The costs of operating and maintenance (O&M) of a solar photovoltaic system represent a very small percentage in relation to its initial cost. Because it is a low cost, it is often not considered in an economic analysis and for this reason the national literature lacks relevant data. NREL annually releases studies to price the costs involved in photovoltaic systems in the USA (FU et al., 2018) and it is used in the simulation tool developed.

This work considers a constant linear loss of annual degradation in the 25 years of useful life analysis according to experimental degradation rates published by (JORDAN et al., 2016; JORDAN; KURTZ, 2013).

The electricity bill for each consumer contains the final price, which is the tariff defined by ANEEL plus the additional tariff flag, plus taxes not included in electricity costs, such as ICMS (Tax on Circulation of Goods and Services), PIS (Social Integration Program) and COFINS (Contribution for Social Security Financing).

This study considered the CIP of the municipality of Rio de Janeiro governed by Law 6,311 / 2017 and corrected annually by the IPCA (Broad Consumer Price Index).

To arrive at the result of the final total monthly tariff TT , the following equation is considered:

$$TT = \frac{CE \frac{TC + BT}{(1 - (ICMS + PIS + COFINS))} + CIP}{CE} \quad (4)$$

Where CE is the energy consumption in the month, TC is the conventional tariff and BT the tariff flag.

However, this is the tariff charged by the distributor for the energy consumed, but it is not the same portion that is remunerated. Taxes and fees like CIP are not remunerated, as they continue to be charged to the consumer. Each state has its own rule regarding the collection of ICMS. In the state of Rio de Janeiro for example, Law No. 8922 of 06/30/2020 exempts ICMS collection by distributors for injected energy. Thus, this work considers the remunerated tariff as follows:

$$TR = \frac{TC + BT}{(1 - ICMS)} \quad (5)$$

3. RESULTS

In order to facilitate the understanding of the results shown here, two different configurations of photovoltaic systems were determined. For this, each has its own consumption profile, equipment used, location and economic data. The solar panel models chosen are currently being widely marketed in Brazil. The consumption profile and geographical coordinates of both configurations seek to represent real consumer units.

Configuration 1 (C1) - It is characterized by a residential system with roof fixing for a large house with 4 to 5 people, located in the Recreio dos Bandeirantes, Rio de Janeiro, RJ.

Table 1 - Simulation parameters of the C1 configuration.

Consumption profile in kWh											
JAN	FEB	MAR	APR	MAY	JUN	JUL	AUG	SEP	OCT	NOV	DEZ
1180	850	800	590	730	600	630	710	800	800	540	720
Geolocation:		Lat	-23,02	Long	-43,46						
Panel model:		Canadian Solar Inc, CS3U-365MS-AG									

Configuration 2 (C2) - It is characterized by a small commercial / industrial system, located in the municipality of Nova Friburgo, RJ.

Table 2 - Simulation parameters of the C2 configuration.

Consumption profile in kWh											
JAN	FEB	MAR	APR	MAY	JUN	JUL	AUG	SEP	OCT	NOV	DEZ
9600	8600	7200	5310	6570	5400	5670	6390	5460	5700	6230	6480
Geolocation:		Lat	-22,29	Long	-42,54						
Panel model:		Jinko Solar Co., Ltd., JKM400M-72HL-V									

3.1 Validation of the developed model

To validate the modeling of the simulation tool developed, the results of annual electricity generation for the C1 and C2 configurations were compared with three different commercial software well established in the market: Pvsyst 7.0, RETScreen Expert 7.0 and PV*Sol Premium 2020. The Graph reveals the comparison results for the C1 configuration.

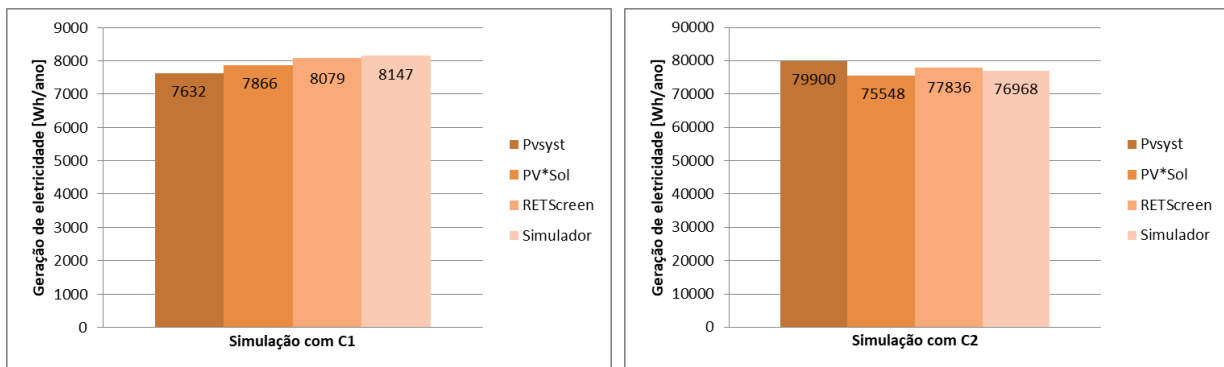


Figure 3 - Annual electricity generation comparison for the simulation tool and commercial software for C1 and C2.

For the C1 configuration, the developed simulation tool obtained generation results higher than the 3 commercial software, but closer to the RETScreen software with a difference of 0.84%. For the PV*Sol and Pvsyst software, there was a difference of 3.57% and 6.75%, respectively. For the C2 configuration, the results were quite different, with the highest generation for the Pvsyst software, followed by RETScreen, a developed simulator and PV*Sol. The generation differences in relation to the developed simulator were 3.81% for Pvsyst software, 1.88% for PV * Sol and 1.13% for RETScreen.

The difference in the results is to be expected, taking into account that the meteorological information obtained in each software is quite different. In the RETScreen and PV*Sol software, both configurations used the meteorological information from Santos Dumont station, from the NASA and MeteoSyn database respectively. This was the only station available for both software in the state of Rio de Janeiro. In Pvsyst, the information was imported from the coordinates specified in the Meteororm database settings. Divergent results are to be expected, as the simulator uses a more accurate database within the locality of the state of RJ. In the same way, each software has its own calculation procedures and loss considerations that also affect the final result. Thus, with these results, it is sufficient to validate the functionality of the developed simulator.

3.2 Tracking models comparison

Four different solar tracking models were compared according to the monthly incident radiation. The simulation was performed for the location of C1. When not varying the angle in the tracking, the angle of inclination was fixed equal to the latitude and the azimuth angle 180° (facing north).

It is observed that clearly the models with two axes and one vertical axis have the best performance results. However, in a few months there is a better performance for the model of a vertical axis. This result is due to the fact that using tracking on two axes, gains are obtained only during days with clear skies. On cloudy days, tracking on two axes does not allow for energy gain and may even reduce the incidence of radiation on panels, as there is less use of diffuse radiation (CABRERA, 2014).

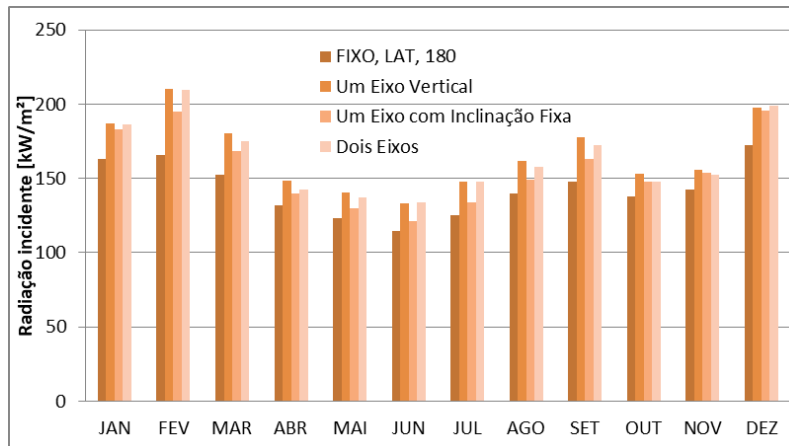


Figure 4 –Comparison between solar tracking models performance.

However, the vast majority of small and medium-sized residential and commercial / industrial systems are installed in roof or floor structures fixed to a certain slope β and azimuthal direction of the surface γ . Thus, it is interesting to study in more detail the variation of these slopes, with the generation of contour surfaces that reveal an optimization problem. For this comparison, hourly data was used directly from INMET stations, to avoid approximations of the correlations that transform the daily average data into hourly data. Three stations were chosen in different regions of Rio de Janeiro: Teresópolis and Cambuci. For these results, Perez's diffuse radiation model was used.

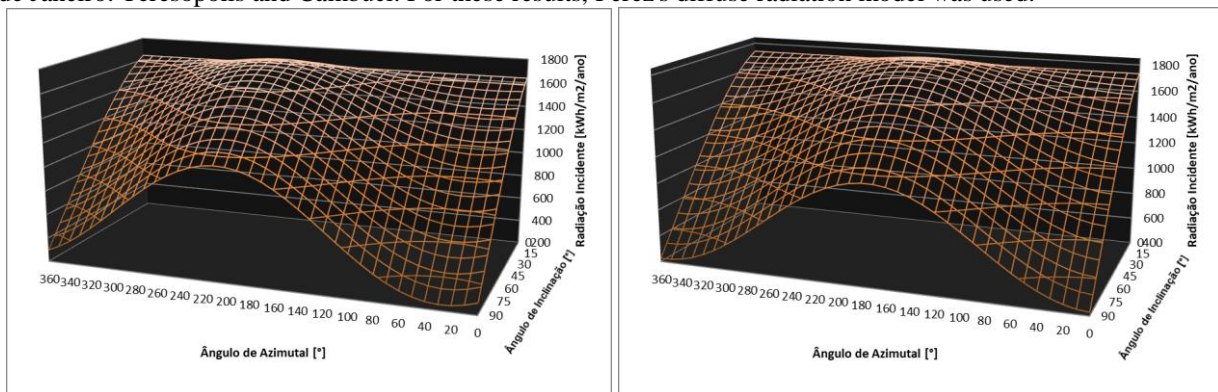


Figure 5 - Result of incident radiation from a fixed system in the municipality of Teresópolis and Cambuci - RJ, varying the azimuth and inclination angles of the panel.

It is observed that, as expected, the graphs present a constant straight line for $\beta = 0$, that is, when the panel is horizontal. Likewise, the results are the same for $\gamma = 0^\circ$ or $\gamma = 360^\circ$, as it corresponds to the panel facing south and presents its minimum values when $\beta = 90^\circ$, that is, vertically. It is interesting to note that, contrary to popular belief, not always directing the panel towards geographic north, that is, $\gamma = 180^\circ$ offers the best performance for the solar panel. And likewise, it is not trivial that the slope of the panel equal to latitude is the optimum point for absorbing incident radiation. These can be used as simplified starting points for design parameters. However, as noted in the graph, the location may offer variations in the incident radiation during the morning and in the afternoon, causing the optimum point to be shifted to the west or east, or even to suggest other optimal slopes for the module.

As noted in (CABRERA, 2014) this difference can be caused by pollution, which affects the continental part on a larger scale than the oceans. Thus, as the release of GHG into the atmosphere occurs mostly starting in the morning until late afternoon, which implies lower concentrations during the early morning. Thus, during the morning, the incident radiation is greater and during the afternoon a higher concentration of gases could cause this difference. However, other climatic and geographical factors could also explain this difference, such as cloud cover and other obstacles on the horizon.

3.3 Georeferenced maps generation

In the literature, it is common to find maps that inform global radiation according to the geographic coordinate. These maps are important for the initial analysis of the places where there is the best use of solar radiation. However, this information should not be decisive in the analysis for investment in a photovoltaic installation. There are several economic variables from each country or state that influence investment analysis. Thus, maps of the economic indicators were generated for configurations C1 and C2, where it is possible to view the differences that exist within the state of Rio de Janeiro.

For the next simulations, the inflation rate was calculated using an average of the IPC Brazil for the past 10 years. The escalation rate of the energy cost is an average of the rate of increase in the cost of the energy tariff over the last 10 years for distributors in Rio de Janeiro. The discount rate is the Regulatory Capital Remuneration Rate of the distribution approved by ANEEL RN n° 882/2020 (ANEEL, 2020).

Figure 6 shows the Competitiveness Index (CI), which is a dimensionless indicator that reflects whether the photovoltaic installation is profitable or not according to the location. If IC is above 1, that is when LCOE is below the tariff paid by the distributor, it means that the installation is viable. It is observed that for the C1 configuration, the CI for the installed systems varies from approximately 2 to 2.7, while for C2 they vary from 2.6 to 3.6. This result reveals that, even with higher installation costs pro kWp, depending on the locality of the state of RJ, the C1 residential system may have a higher CI than C2. Thus, the choice of location, even within a state, can be crucial to obtain better financial returns on investment.

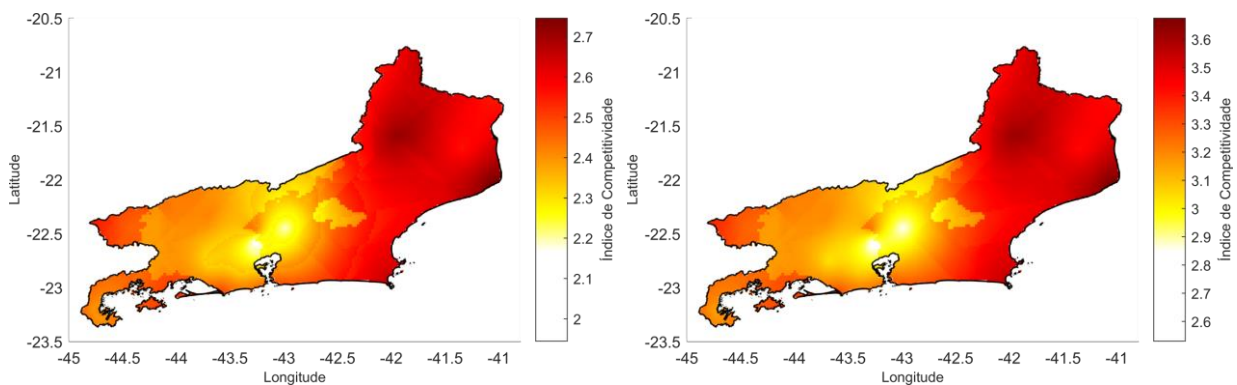


Figure 6 –Competitiveness Index map for C1 and C2.

The LCOE is the most used indicator in the literature to compare the financial viability of projects with different configurations and energy sources. However, it does not prove to be entirely adequate, as it does not take into consideration the remuneration tariff adopted by the local energy distributor. It is observed that the boundaries of the distributors in this case are not observed. Thus, the CI is a more suitable indicator for comparing the feasibility of photovoltaic projects in different locations. See in Figure 7.

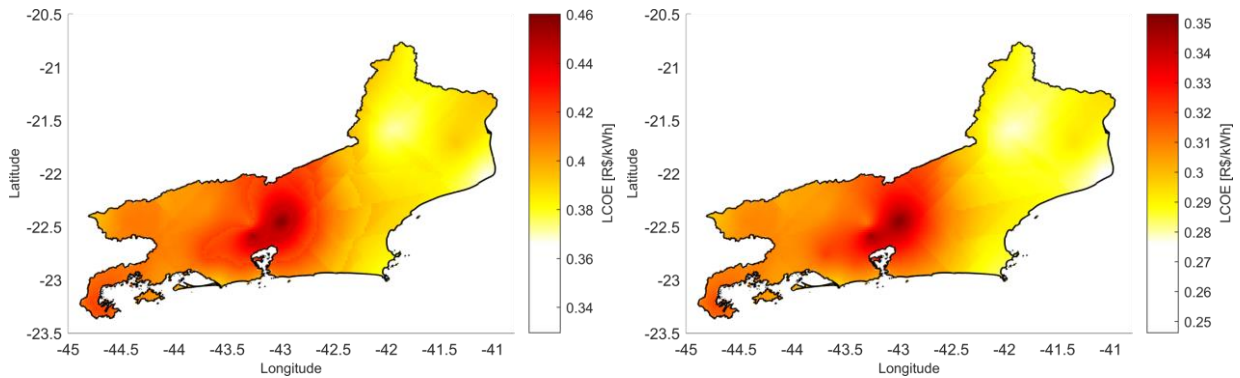


Figure 7 – Levelized Cost of Electricity map for C1 and C2.

Figure 8 shows the number of panels for C1 and C2, respectively. This map clearly demonstrates that even within the state of RJ, it is possible to design systems for the same generation, but with a different number of panels for the same demand. In other words, a lower system power can be sized to meet the same demand as a system with greater power depending on its location. The C1 configuration, for example, varies from 11 to 16 panels and the C2 configuration from 100 to 140 panels, showing that within RJ a configuration with up to 45% less power, can generate the same energy needed to supply the demand for a unit consumer.

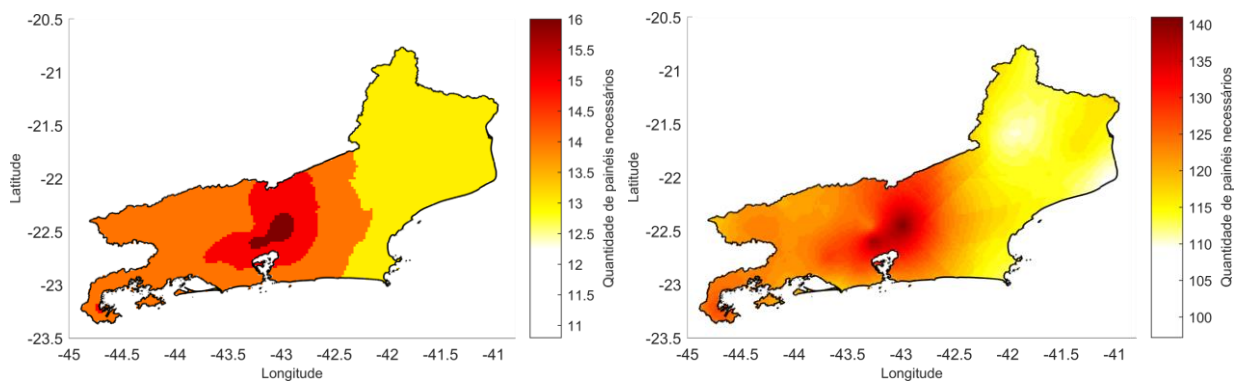


Figure 8 - Photovoltaic module necessary quantity map for C1 and C2.

The maps of the amount of tCO₂ avoided in the atmosphere for C1 and C2 (Figure 9), demonstrate the environmental benefits of photovoltaic projects throughout their useful life, as they deal with renewable energy and do not depend on fossil fuels. It is interesting to note that although this indicator is directly linked to the amount of energy generated by the dimensioned system, there is a small difference in the shape of waves along the territorial extension of the state of RJ. This small difference is linked to the fact that the relationship between dimensioning the number of panels and the amount of energy generated. Because the simulator, at each geographical coordinate, seeks the number of panels necessary to generate the energy as close as possible to the energy demand defined by consumption, resulting in this small variation across the territory. This result reveals that, despite little difference, a system installed in a location with worse financial viability indicators, can be as good as, or better, environmentally, than the one installed in a more financially adequate location.

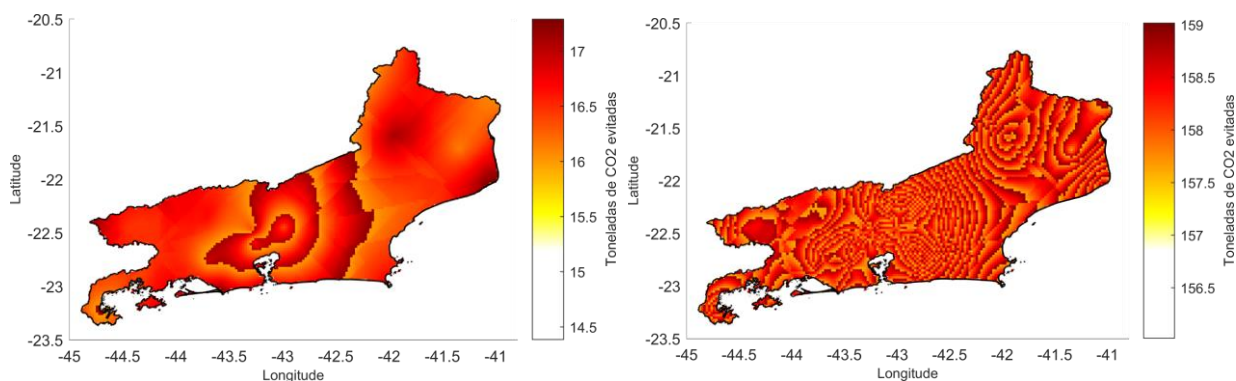


Figure 9 - Map of the amount of tCO₂ avoided in the atmosphere for C1 and C2

4. CONCLUSION

This work concluded the development of a robust algorithm for dimensioning solar photovoltaic systems, using a reliable database for radiation, wind speed and temperature in the state of Rio de Janeiro. It was possible to validate the developed model, comparing the generation results with commercial software well established in the market.

With its proven effectiveness, different tracking models were compared, showing the difference in results expected for each model used. It was also possible to carry out a more detailed analysis of fixed systems on roofs, reaching interesting results.

With that, the main objective was reached, performing simulations for each geographic coordinate of the computational grid, generating georeferenced maps. These maps proved to be an important tool for technical, economical and environmental assessment of solar photovoltaic systems in a given region.

5. REFERENCES

- ANEEL. **Resolução Normativa nº 482, de 17 de abril de 2012 (atualizada)**, 2017.
- ANEEL. **Proret - Submódulo 2.4, revisão 4.1. Remuneração de Capital da Distribuição.**, 2020.
- BRAUN, J. E.; MITCHELL, J. C. Solar geometry for fixed and tracking surfaces. **Solar Energy**, v. 31, n. 5, p. 439–444, 1983.
- CABRERA, F. C. A. **Avaliação da disponibilidade do recurso solar no Estado do Rio de Janeiro**. [s.l.] PUC-Rio., 2014.
- COLLARES-PEREIRA, M.; RABL, A. The average distribution of solar radiation-correlations between diffuse and hemispherical and between daily and hourly insolation values. **Solar Energy**, v. 22, n. 2, p. 155–164, 1979.
- DUFFIE, J. A.; BECKMAN, W. A. **Solar Engineering of Thermal Processes, Photovoltaics and Wind**. 5th Edition ed. Hoboken, New Jersey: [s.n.].
- ERBS, D. G.; KLEIN, S. A.; DUFFIE, J. A. Estimation of the diffuse radiation fraction for hourly, daily and monthly-average global radiation. **Solar Energy**, v. 28, n. 4, p. 293–302, 1982.
- FU, R. et al. U . S . Solar Photovoltaic System Cost Benchmark : Q1 2018. **National Renewable energy Laboratory**, 2018.
- GARG, H. P.; GARG, S. N. Improved correlation of daily and hourly diffuse radiation with global radiation for Indian stations. **Solar and Wind Technology**, v. 4, n. 2, p. 113–126, 1987.
- GREENER. **Estudo Estratégico: Mercado Fotovoltaico GD**, 2020. Disponível em:
<<http://greener.greener.com.br/estudo-gd-1sem2019>>
- GUEYMARD, C. Monthly averages of the daily effective optical air mass and solar related angles for horizontal or inclined surfaces. **Journal of Solar Energy Engineering, Transactions of the ASME**, v. 108, n. 4, p. 320–324, 1986.
- GUEYMARD, C. Prediction and performance assessment of mean hourly global radiation. **Solar Energy**, v. 68, n. 3, p. 285–303, 2000.
- IQBAL, M. **An Introduction to Solar Radiation**. 1983.
- JORDAN, D. C. et al. Compendium of photovoltaic degradation rates. **Progress in Photovoltaics: Research and Applications**, 2016.

- JORDAN, D. C.; KURTZ, S. R. Photovoltaic degradation rates - An Analytical Review. **Progress in Photovoltaics: Research and Applications**, v. 21, n. 1, p. 12–29, 2013.
- LIU, B. Y. H.; JORDAN, R. C. The long-term average performance of flat-plate solar-energy collectors. **Solar Energy**, v. 7, n. 2, p. 53–74, 1963.
- MME/EPE. **Plano Decenal de Expansão de Energia 2029** Empresa de Pesquisa Energética. [s.l: s.n.].
- NATURAL RESOURCES CANADA. **Clean Energy Project Analysis**. [s.l: s.n.].
- NEWELL, T. A. Simple models for hourly to daily radiation ratio correlations. **Solar Energy**, 1983.
- PEREZ, R. et al. Modeling daylight availability and irradiance components from direct and global irradiance. **Solar Energy**, v. 44, n. 5, p. 271–289, 1990.
- PORTAL SOLAR. **Painel Solar - Preços e Custos de Instalação**. Disponível em:
<<https://www.portalsolar.com.br/painel-solar-precos-custos-de-instalacao.html>>.
- REINDL, D. T.; BECKMAN, W. A.; DUFFIE, J. A. Evaluation of hourly tilted surface radiation models. **Solar Energy**, v. 45, n. 1, p. 9–17, 1990.
- SHORT, W.; PACKEY, D.; HOLT, T. A manual for the economic evaluation of energy efficiency and renewable energy technologies. **Renewable Energy**, v. 95, n. March, p. 73–81, 1995.
- SPENCER, J. W. Fourier series representation of the position of the sun. v. 2, p. 172, 1971.
- WHILLIER, A. The determination of hourly values of total solar radiation from daily summations. **Archiv für Meteorologie, Geophysik und Bioklimatologie Serie B**, v. 7, n. 2, p. 197–204, 1956.

6. RESPONSIBILITY NOTICE

The authors are the only responsible for the printed material included in this paper.